Cavity quantum electrodynamics with quantum dots in microcavities

Gudat, J.

Chapter 7

Schemes in the Weak-Coupling Cavity QED Regime

This chapter is based on the following publication: *CNOT and Bell-state analysis in the weak-coupling cavity QED regime* (C. Bonato, F. Haupt, S. S. R. Oemrawsingh, J. Gudat, D. Ding, M. P. van Exter, and D. Bouwmeester, Phys. Rev. Lett. 104, 160503 (2010)) [26].

In Chap. 1 we described general ideas on how to obtain single-photon single-electron interactions. One important aspect is the possibility to realize such interactions in the weak-coupling cavity QED regime where experimental feasibility is much simpler compared to requirements of the strong-coupling regime. The aim of this chapter is to design an interface based on spin selective photon reflection from the cavity that allows implementation of a controlled NOT (CNOT) gate which serves as the essential component of a quantum computer. Additionally we describe a scheme for a multiphoton entangler and a photonic Bell-state analyzer. Finally, we analyze the experimental feasibility of these schemes and conclude that they can be implemented with current technology.

7.1 Introduction

Hybrid (photon-matter) systems can be used for quantum information applications and to effectively enable strong nonlinear interactions between single photons [164–166]. Several systems have been identified as candidates for local matter qubits, for example, atoms [167, 168], ions [169], superconducting circuits [170, 171], and semiconductor QDs [136, 154, 172], and their coupling strengths to optical modes have been investigated.

Quantum information protocols based on cavity QED often require the system to operate in the strong-coupling regime [164, 173–175], where the vacuum Rabi frequency of the dipole g exceeds both the cavity and dipole decay rates. However, in the bad cavity limit, where g is smaller than the cavity decay rate, the coupling between the radiation and the dipole can drastically change the cavity reflection and transmission properties [54, 176, 177], allowing quantum information schemes to operate in the weak-coupling regime. We exploit this regime, using spin selective dipole coupling, for a system consisting of a single electron charged self-assembled GaAs/InAs QD in a micropillar resonator [24, 42]. The potential of this system has also been recognized in [178]. We first show that this specific system can lead to a quantum CNOT gate with the confined electron spin as the control qubit and the incoming photon spin as the target qubit. We apply the CNOT gate to generate multiphoton entangled states. We then construct a complete two-photon Bell-state analyzer (BSA). Complete deterministic BSA is an important prerequisite for many quantum information protocols like superdense coding, teleportation, or entanglement swapping. It cannot be performed with linear optics only [179], while it can be done using nonlinear optical processes [180] (with low efficiency) or employing measurement-based nonlinearities in nondeterministic schemes [113]. Deterministic complete BSA has been shown in a scheme which is conceptually different from the one presented here, exploiting entanglement in two or more degrees of freedom of two photons [181, 182]. We conclude with a discussion on the experimental feasibility of the proposed schemes.

7.2 Optical selection rules

In the limit of a weak incoming field, a cavity with a dipole behaves like a linear beam splitter whose reflection (r) and transmission (t) are given by [54]

$$r = \frac{i\xi}{1 + i\xi} \tag{7.1}$$

$$t = -\frac{1}{1 + i\xi} \tag{7.2}$$

$$\xi = \frac{\Delta w \delta}{\kappa} - \frac{\Gamma}{2\Delta w} \tag{7.3}$$

where Δw is the frequency detuning between the photon and the dipole transition, δ is the detuning between the cavity mode and the dipole transition, κ describes the coupling to the input and output ports, and Γ is the relaxation

time of the dipole ($\Gamma = 2g^2/\kappa$). In the following, we consider the case of a dipole tuned into resonance with the cavity mode ($\delta = 0$), probed with resonant light ($\Delta w = 0$). If the radiation is not coupled to the dipole transition ($g = 0$, $\xi \to 0$) the cavity is transmissive, while a coupled system ($g \neq 0$, $\xi \to \infty$) can exhibit reflection of the field incident on the cavity.

We now consider the dipole transitions associated with a singly charged GaAs/InAs QD. The four relevant electronic levels are shown in Fig. 7.1 and have been described in detail in Chap. 6. Summarizing, there are two optically allowed transitions between the electron state and the trion state (bound state of two electrons and a hole). The single electron states have $J_z = \pm 1/2$ spin ($|\uparrow\rangle$,$|\downarrow\rangle$) and the holes have $J_z = \pm 3/2$ ($|\Uparrow\rangle$,$|\Downarrow\rangle$) The quantization axis for angular momentum is the z axis because the QD confinement potential is much tighter in the z (growth) direction than in the transversal direction due to the QD geometry. In a trion state, the two electrons form a singlet state and therefore have total spin zero, which prevents electron-spin interactions with the hole spin. This makes the two dipole transitions, one involving a $s_z = +1$ photon and the other a $s_z = -1$ photon, degenerate in energy, which is a crucial requirement for achieving entanglement between photon spin and electron spin.

The spin s_z of the photons in the fundamental micropillar modes is also naturally defined with respect to the z axis. Photon polarization is commonly defined with respect to the direction of propagation, and this causes the handedness of circularly-polarized light to change upon reflection, whereas the absolute rotation direction of its electromagnetic fields does not change. We will therefore label the optical states by their circular polarization (labels $\mid L\rangle$ and $\mid R\rangle$) and by a superscript arrow to indicate their propagation direction along the z axis. According to this definition, the photon spin s_z remains unchanged upon reflection and the dipole-field interaction is determined only by the relative orientation of the photon spin with respect to the electron spin (see Fig. 7.1). This level scheme is idealized and does not include the nonradiative coupling between the levels, in particular, due to spin interactions with the surrounding nuclei, which lead to spin dephasing [153].

Consider a photon in the state $\mid R^{\uparrow}\rangle$ and $\mid L^{\downarrow}\rangle$ ($s_z = +1$). If the electron spin is in the state $|\uparrow\rangle$, there is a dipole interaction and the photon is reflected by the cavity. Upon reflection, both the photon polarization and propagation direction are flipped and the input states are transformed, respectively, into the states $\mid L^{\downarrow}\rangle$ and $\mid R^{\uparrow}\rangle$. When the electron spin is in the $|\downarrow\rangle$ state, the photon states are transmitted through the cavity and acquire a π mod 2π phase shift relative to a reflected photon state. In the case of a $|\uparrow\rangle$ electron-spin state, the

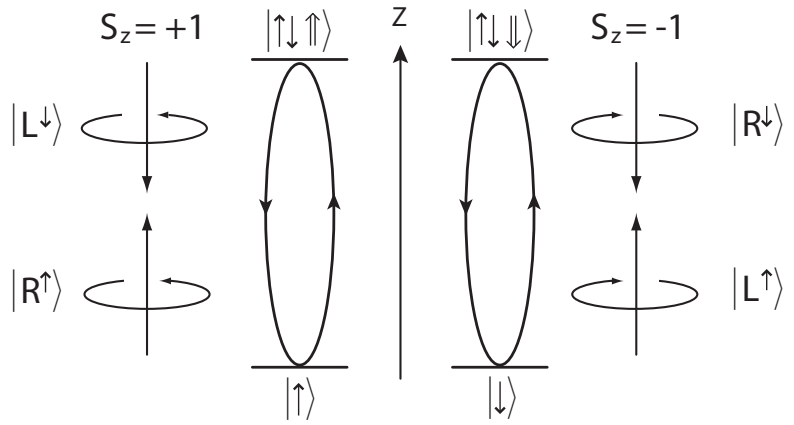

Figure 7.1: *Relevant energy levels and optical selection rules for GaAs/InAs QDs.*

interaction between the photon and the cavity is described by

$$\begin{array}{ll} \mid R^{\uparrow},\uparrow\rangle \mapsto \mid L^{\downarrow},\uparrow\rangle & \mid L^{\downarrow},\uparrow\rangle \mapsto \mid R^{\uparrow},\uparrow\rangle \\ \mid R^{\downarrow},\uparrow\rangle \mapsto -\mid R^{\downarrow},\uparrow\rangle & \mid L^{\uparrow},\uparrow\rangle \mapsto -\mid L^{\uparrow},\uparrow\rangle \end{array} \tag{7.4}$$

In the same way, the states $\mid R^{\downarrow}\rangle$ and $\mid L^{\uparrow}\rangle$ ($s_z = -1$) are reflected if the electron-spin state is $|\downarrow\rangle$ and are transmitted through the cavity when the spin is $|\uparrow\rangle$.

7.3 CNOT gate

A first application of the cavity-induced photon-spin electron-spin interface is the conditional preparation of either the $|\uparrow\rangle$ or the $|\downarrow\rangle$ electron-spin state. Suppose that a $\mid R^{\uparrow}\rangle$ photon is incident on the cavity and the electron spin is in the state $\mid \psi_{el}\rangle = \alpha\,|\uparrow\rangle + \beta\,|\downarrow\rangle$. Through the interaction we obtain the entangled state $\mid \psi\rangle = \alpha \mid L^{\downarrow},\uparrow\rangle - \beta \mid R^{\uparrow},\downarrow\rangle$. The detection of a photon reflected (transmitted) by the cavity projects the electron spin onto the $|\uparrow\rangle$ ($|\downarrow\rangle$) state. Electron-spin projection along the x or y axis is not possible using photons propagating along the z axis. Figure 7.2 shows how the interface can be used to construct a CNOT gate with the control bit the spin of the electron and the target bit the spin of the photon. Consider an incident photon in the polarization state $\mid \psi_{ph}\rangle = \alpha \mid R\rangle + \beta \mid L\rangle$ and an electron spin in the

state $\mid \psi_{el}\rangle = \gamma \mid\uparrow\rangle + \delta \mid\downarrow\rangle$. The polarizing beam splitter in the circular basis (c-PBS) separates the input photon state into $\alpha \mid R^{\downarrow}\rangle$, propagating in mode C, and $\beta \mid L^{\uparrow}\rangle$, propagating in mode B. Eventually all photon components, either transmitted or reflected by the cavity, end up in output port D due to the polarization flip on reflection and the properties of the c-PBS. The circuit in Fig. 7.2 transforms the input state $\mid \psi\rangle_{in} = \mid \psi_{ph}\rangle \otimes \mid \psi_{el}\rangle$ into

$$\mid \psi\rangle_{out} = \gamma \mid\uparrow\rangle [\alpha \mid R\rangle + \beta \mid L\rangle] + \delta \mid\downarrow\rangle [\alpha \mid L\rangle + \beta \mid R\rangle] \tag{7.5}$$

provided that the phase differences in the four possible optical trajectories are equal mod 2π. To this end, a π phase shift has to be included in one arm so that the two photon trajectories passing through the cavity (in opposite directions) pick up a π phase relative to the two possible reflective trajectories. Together with the intrinsic π phase shift upon cavity transmission, all trajectories are in phase in the output port of the c-PBS (note that a PBS can always be constructed such that no relative phase shifts between reflected and transmitted components occur). Each arm needs to comprise of an even number of mirrors, so that no net flip of polarization handedness results. Equation (7.5) shows that the circuit operates as a CNOT gate, where the target photon state remains unaltered when the control electron spin is $|\uparrow\rangle$, and flips if the electron spin is $|\downarrow\rangle$

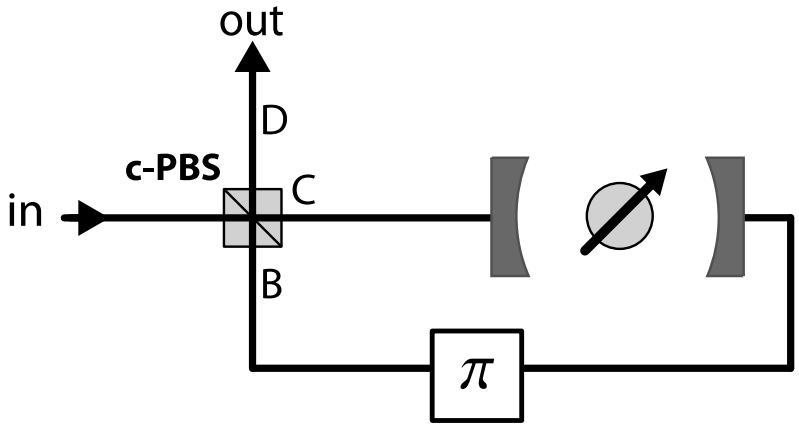

Figure 7.2: *CNOT gate scheme.*

The CNOT gate, a universal quantum gate providing entanglement between target and control qubit, has numerous applications in the field of quantum information science [183]. For example, it can be used to mediate entangling and disentangling operations on two or more photons. Suppose the

electron-spin state is prepared in the $1/\sqrt{2}(|\uparrow\rangle + |\downarrow\rangle)$ state and two uncorrelated photons, in the factorizable state $|\,\psi_0\rangle = (\alpha_1 \mid R_1\rangle + \beta_1 \mid L_1\rangle) \times (\alpha_2 \mid R_2\rangle + \beta_2 \mid L_2\rangle)$, are sent through the input port one after the another. After interaction with the CNOT gate, both photons will emerge in succession through the output port D, in the state

$$\begin{aligned} |\,\psi\rangle &= |+\rangle\{(\alpha_1\alpha_2 + \beta_1\beta_2) \mid \varphi_+\rangle + (\alpha_1\beta_2 + \beta_1\alpha_2) \mid \psi_+\rangle\} \\ &+ |-\rangle\{(\alpha_1\alpha_2 - \beta_1\beta_2) \mid \varphi_-\rangle + (\alpha_1\beta_2 - \beta_1\alpha_2) \mid \psi_-\rangle\} \end{aligned} \tag{7.6}$$

where $|\,\psi^{(\pm)}\rangle$ and $|\,\varphi^{(\pm)}\rangle$ are the Bell states

$$|\,\varphi^{(\pm)}\rangle = \frac{1}{\sqrt{2}}\,[|\,R_1\rangle \mid R_2\rangle \pm |\,L_1\rangle \mid L_2\rangle] \tag{7.7}$$

$$|\,\psi^{(\pm)}\rangle = \frac{1}{\sqrt{2}}\,[|\,R_1\rangle \mid L_2\rangle \pm |\,L_1\rangle \mid R_2\rangle] \tag{7.8}$$

and $|\pm\rangle = \frac{1}{\sqrt{2}}(|\uparrow\rangle \pm |\downarrow\rangle)$. This state is a three-particle entangled state and is written in the electron-spin detection basis that will, for given values of α's and of β's, result in a specific two-photon entangled state after the electron-spin projection measurement. More photons can be entangled in order to create multiphoton entanglement. For example, feeding the gate with a stream of right-hand circularly-polarized photons, and projecting the spin state on the $|\pm\rangle$ basis, after all the photons have interacted with the spin, N-photon Greenberger-Horne-Zeilinger states

$$|\,\mathrm{GHZ}\rangle = \frac{1}{\sqrt{2}}\left[|\,L\rangle^{\otimes N} + |\,R\rangle^{\otimes N}\right] \tag{7.9}$$

can be created. Such states have important applications, like quantum secret sharing and multiparty quantum networking.

7.4 Bell-state analyzer

The second scheme presented in this chapter is sketched in Fig. 7.3. The aim is to perform a deterministic and complete Bell-state analysis on an input of two subsequent photons. Consider first the two-photon Bell states in equation (7.8). $|\,\varphi\rangle$ states can be distinguished from $|\,\psi\rangle$ states by measuring two-photon correlations in the $\{|\,R\rangle, |\,L\rangle\}$ basis. Determining the $\pm$ sign in equation (7.8) would require correlation measurements in a linearized polarization $\{|\,H\rangle, |\,V\rangle\}$ basis, which is incompatible with the previous measurement. Our idea is to entangle the two photons to be analyzed with an electron spin such that each joint measurement result for the three-particle state can be uniquely

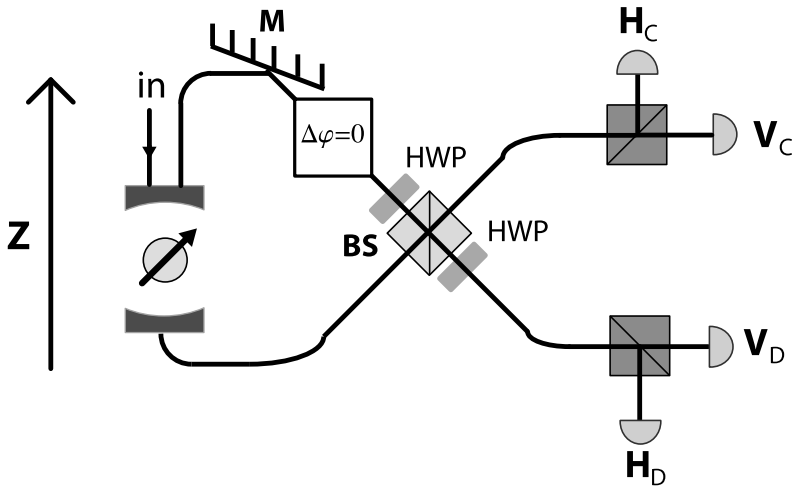

Figure 7.3: *Bell-state analyzing scheme.*

associated with a single photonic Bell state.

Suppose the electron spin is prepared in $\mid +\rangle$. The two photons come in succession to the cavity and the reflected and transmitted paths are combined with equal path length on a 50/50 beamsplitter (BS). The reflected path can be separated from the input path by means of a polarization-maintaining fiber circulator. We assume the BS will not change the polarization on the reflected port: this can be implemented by the two half-wave plates (HWP). If the input two-photon state is $\mid \psi^{(\pm)}\rangle$, then the state at the output ports of the BS is (taking into account that reflection from the mirror M interchanges $\mid R\rangle$ and $\mid L\rangle$)

$$\frac{1}{2}\{i[\mid \psi^{(\pm)}_{CC}\rangle + \mid \psi^{(\pm)}_{DD}\rangle] \mid +\rangle + [\mid \psi^{(\mp)}_{CD}\rangle - \mid \psi^{(\mp)}_{DC}\rangle] \mid -\rangle\} \tag{7.10}$$

where $\mid \psi^{(\pm)}_{ij}\rangle = \frac{1}{\sqrt{2}}[\mid R_{1i}\rangle \mid L_{2j}\rangle \pm \mid L_{1i}\rangle \mid R_{2j}\rangle]$. For an input $\mid \varphi^{(\pm)}\rangle$ state we obtain

$$\frac{1}{2}\{[\mid \varphi^{(\mp)}_{CC}\rangle - \mid \varphi^{(\mp)}_{DD}\rangle] \mid -\rangle + i[\mid \varphi^{(\pm)}_{CD}\rangle + \mid \varphi^{(\pm)}_{DC}\rangle] \mid +\rangle\}. \tag{7.11}$$

In case both photons go out the same port (either CC or DD), measuring the electron-spin state we can identify whether the two-photon input state was $\mid \psi\rangle$ type (corresponding to spin $\mid +\rangle$) or $\mid \varphi\rangle$ type (corresponding to spin $\mid -\rangle$). Measuring the two photons in the $\{\mid H\rangle, \mid V\rangle\}$ polarization basis, it is then possible to distinguish between $\mid \varphi^{(+)}\rangle$ and $\mid \varphi^{(-)}\rangle$ and between $\mid \psi^{(+)}\rangle$ and $\mid \psi^{(-)}\rangle$. Similar considerations are valid for the case where the photons exit the system through different ports. Therefore, each measurement result (con-

Table 7.1: *Output results for each photonic Bell state. Each result (consisting of polarization in the* $\{|H\rangle, |V\rangle\}$ *basis and output port for the photon and spin in the* $\{|+\rangle, |-\rangle\}$ *basis for the electron in the QD) is uniquely associated with one photonic Bell state.*

State	Results				
$\|\psi^{(+)}\rangle$	$\|+\rangle$:	$\|H_1^C, H_2^C\rangle$	$\|V_1^C, V_2^C\rangle$	$\|H_1^D, H_2^D\rangle$	$\|V_1^D, V_2^D\rangle$
	$\|-\rangle$:	$\|H_1^C, V_2^D\rangle$	$\|V_1^C, H_2^D\rangle$	$\|H_1^D, V_2^C\rangle$	$\|V_1^D, H_2^C\rangle$
$\|\psi^{(-)}\rangle$	$\|+\rangle$:	$\|H_1^C, V_2^C\rangle$	$\|V_1^C, H_2^C\rangle$	$\|H_1^D, V_2^D\rangle$	$\|V_1^D, H_2^D\rangle$
	$\|-\rangle$:	$\|H_1^C, H_2^D\rangle$	$\|V_1^C, V_2^D\rangle$	$\|H_1^D, H_2^C\rangle$	$\|V_1^D, V_2^C\rangle$
$\|\varphi^{(+)}\rangle$	$\|+\rangle$:	$\|H_1^C, V_2^C\rangle$	$\|V_1^C, H_2^C\rangle$	$\|H_1^D, V_2^D\rangle$	$\|V_1^D, H_2^D\rangle$
	$\|-\rangle$:	$\|H_1^C, H_2^D\rangle$	$\|V_1^C, V_2^D\rangle$	$\|H_1^D, H_2^C\rangle$	$\|V_1^D, V_2^C\rangle$
$\|\varphi^{(-)}\rangle$	$\|+\rangle$:	$\|H_1^C, H_2^C\rangle$	$\|V_1^C, V_2^C\rangle$	$\|H_1^D, H_2^D\rangle$	$\|V_1^D, V_2^D\rangle$
	$\|-\rangle$:	$\|H_1^C, V_2^D\rangle$	$\|V_1^C, H_2^D\rangle$	$\|H_1^D, V_2^C\rangle$	$\|V_1^D, H_2^C\rangle$

sisting of photon $\{|H\rangle, |V\rangle\}$ polarization and output port for the two photons and spin on the $\{|+\rangle, |-\rangle\}$ basis for the electron) is uniquely associated with a single photonic Bell state. A summary of the possible measurement results for each input Bell state is given in Table 7.1.

7.5 Experimental feasibility

Phase stability is required in the two paths arms from the cavity to the BS, but no interferometric stability is needed between the two photons since their interaction is only through the electron spin. A performance parameter for a realistic system is the difference Δ between the transmission for the uncoupled and coupled cavity. From [54], in the simple case of no exciton dephasing and assuming the dipole leak to be equal to its emission rate in vacuum:

$$\Delta = T_{max} - T_{min} = \left(\frac{Q}{Q_0}\right)^2 \left[1 - \left(\frac{1}{1+F_P}\right)^2\right] \tag{7.12}$$

where Q_0 is the quality factor of the cavity due to the output coupling, Q is the cavity quality factor including the leaks ($Q \leq Q_0$), and F_P is the Purcell factor of the two-level system. For a micropillar cavity with oxide apertures [24] the optical losses due to radiation ($\alpha_{rad} = 1.7 \times 10^{-3} cm^{-1}$) and aperture scattering ($\alpha_{scat} = 1.7 cm^{-1}$) are much smaller than the photon escape losses through the top mirror ($\alpha_m = 13.9 cm^{-1}$): for these values $T_{max} = (Q/Q_0)^2 \approx 0.8$. Purcell factors around $F_P = 6$ can be reached with these cavities [55], for

which $\Delta \approx 0.78$. In general the value of Δ can be increased by reducing the cavity losses and increasing the Purcell factor and the dipole lifetime. Oxide-apertured micropillar cavities also have a very high coupling efficiency between the light and the QD [55], can incorporate intracavity electron charging, and can be made polarization degenerate [71] Optical fibers may be glued on both sides, following etching of the back wafer substrate to reduce losses. Other kinds of microcavities, like photonic crystals and microdisks, can be considered as well, but light coupling is in general inefficient and polarization degeneracy is extremely difficult to achieve, due to the intrinsic anisotropy of such structures.

A crucial aspect is the preparation of electron-spin superpositions ($|\pm\rangle$). Significant progress has been made in the manipulation of single electron spins [138, 144, 184, 185]. Spin manipulation typically requires Zeeman splitting of the spin ground states, which may be achieved with a magnetic field or through the optical Stark effect. Ground state degeneracy, with a Zeeman splitting less than the photon bandwidth, has to be restored in the implementation of quantum information protocols. Ultrafast spin manipulation through the ac-Stark effect, potentially in addition to a weak magnetic field (as shown in [144]), seems more promising for our purposes than preparation involving strong magnetic fields, whose modulation is extremely challenging on time scales shorter than the spin coherence time. Quantum optical applications, such as the photon entangling gate and BSA, require the phase of spin superposition to be constant over the times of interaction with different photons. The dephasing time is typically around $5-10$ ns [10,144] but can be increased by several orders of magnitude by spin echo techniques and manipulations of the nuclear spins [32, 184, 186–189].

Finally, we point out that the combination of conditional spin preparation and probing based on spin-state selective reflection could be used to investigate the dynamics of the QD electron-spin state [129].

7.6 Conclusion

In conclusion, we have introduced a quantum interface between a single photon and the spin state of an electron trapped in a QD, based on cavity QED in the weak-coupling regime. We proposed as possible applications: a spin-photon CNOT gate, a multiphoton entangled state generator, and a photonic Bell-state analyzer.